

# Mass-Dependent Kinematics in Orion Nebula Cluster as Tracers of Formation and Evolution

Lingfeng Wei<sup>1</sup>, Quinn Konopacky<sup>1</sup>, Chris Theissen<sup>1</sup>, Jessica Lu<sup>2</sup>, Dongwon Kim<sup>2</sup>

1. Center for Astrophysics and Space Sciences, University of California, San Diego.

2. Department of Astronomy, University of California, Berkeley.

UC San Diego

CASS

## Overview: Star Cluster Formation and Evolution

**Background:** The kinematics of star clusters, where most stars are born, provide valuable insights in the processes of their formation and evolution. The Orion Nebula Cluster (ONC), being the closest (~389 pc) massive star cluster with active star formation is an ideal target for such a study. Hydrodynamical simulations suggest that stars can form in dense gas filaments via gravitational fragmentation<sup>1</sup>. We hope to unveil if the stars in the ONC are born in this way.

**Aims:** Analyze the mass-dependent kinematics around the ONC core, which is packed with young stars and experiencing most of the interactions within the cluster; Verify the gravitational fragmentation star formation mechanism by observing the correlation between relative velocity and stellar mass.

**Sources:** A total number of 246 low-mass stars<sup>2</sup> within 4' (0.45 pc) of the ONC core, including sources observed by Keck<sup>3</sup>, Hubble Space Telescope (HST)<sup>4</sup>, and SDSS/APOGEE<sup>5, 6</sup>.

**Instrument:** K-band infrared spectrum using NIRSPEC with Adaptive Optics (NIRSPA0)<sup>7, 8</sup> on Keck II.

**Data:** NIRSPEC data, APOGEE data, proper motion measurements<sup>4</sup>.

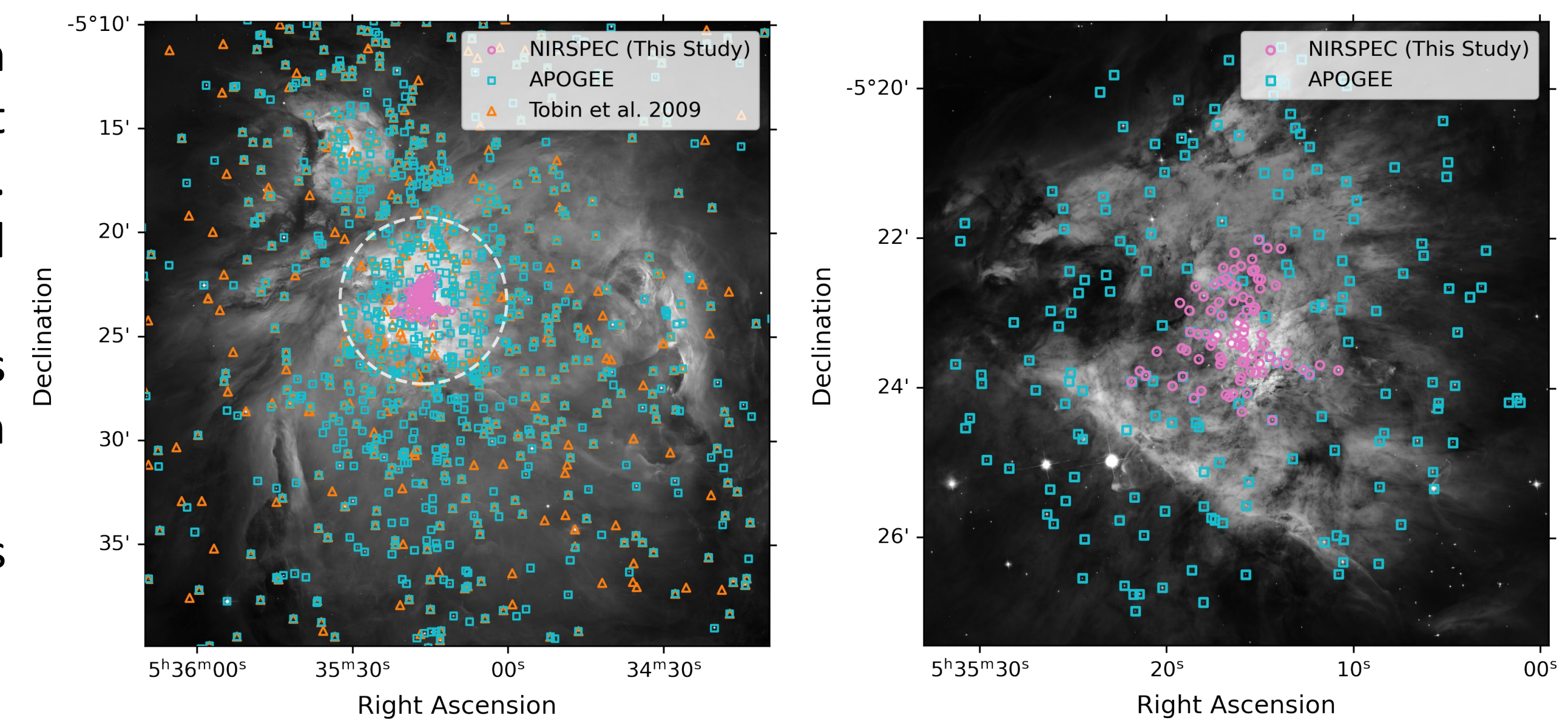


Fig. 1. Sky map of sources near the ONC core in previous studies and this work.

## Method: Spectrum Forward Modeling and Mass Interpolation

1. Spectra are reduced using a modified version of NIRSPEC Data Reduction Pipeline (NSDRP).
2. Spectra of each source are normalized and median combined to reduce white noise.
3. Each spectrum is forward modeled by the PHOENIX stellar model<sup>9</sup> to fit for stellar, telluric, and instrumental parameters using the Spectral Modeling Analysis and RV Tool (SMART)<sup>10, 11</sup>.
4. Masses are then interpolated from multiple stellar evolutionary models<sup>12-15</sup> using the effective temperature assuming an age of  $2 \pm 1$  Myr<sup>16</sup>.

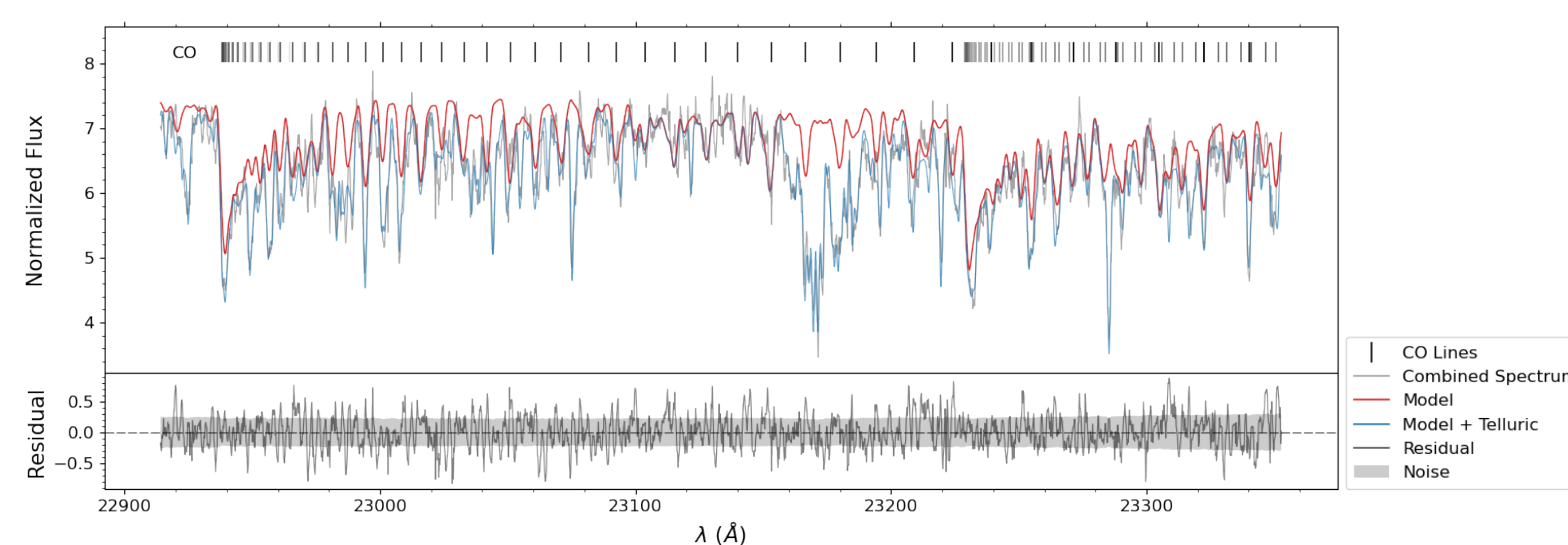


Fig. 2. The spectrum and best-fit atmospheric model of HC2000 172 in order 33.

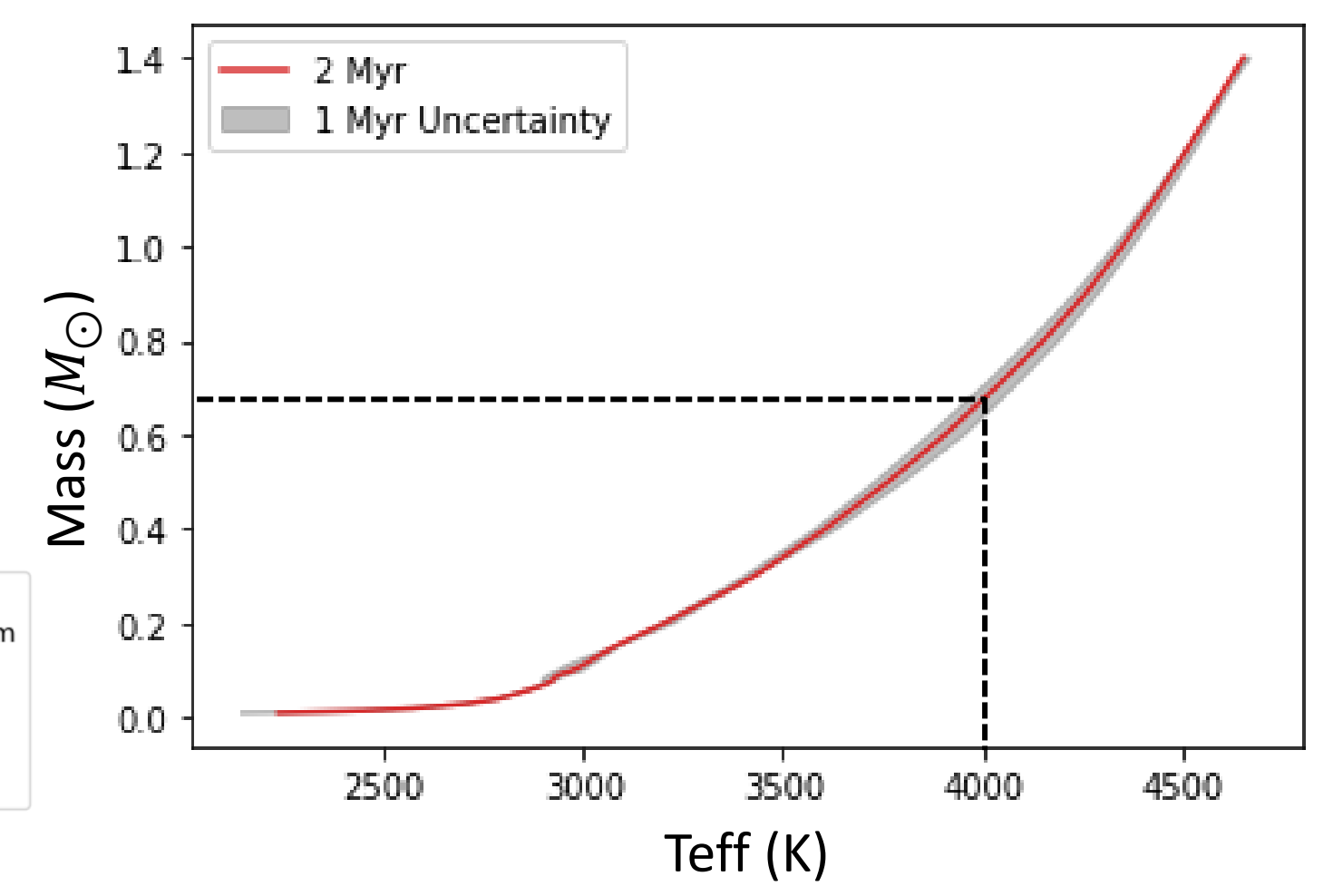


Fig. 3. Mass interpolation based on Baraffe stellar evolutionary model<sup>13</sup>.

## Results: A Test of Star Formation Theory

**Fig. 4** shows the 3-D kinematics map constructed with the radial velocity (RV) modeled from spectra and proper motions measured by the HST. The peak at 90° between the transverse velocities and the displacement vectors from the ONC center suggests that the cluster is undergoing a counter-clockwise rotation, confirming the finding in a previous study<sup>3</sup>.

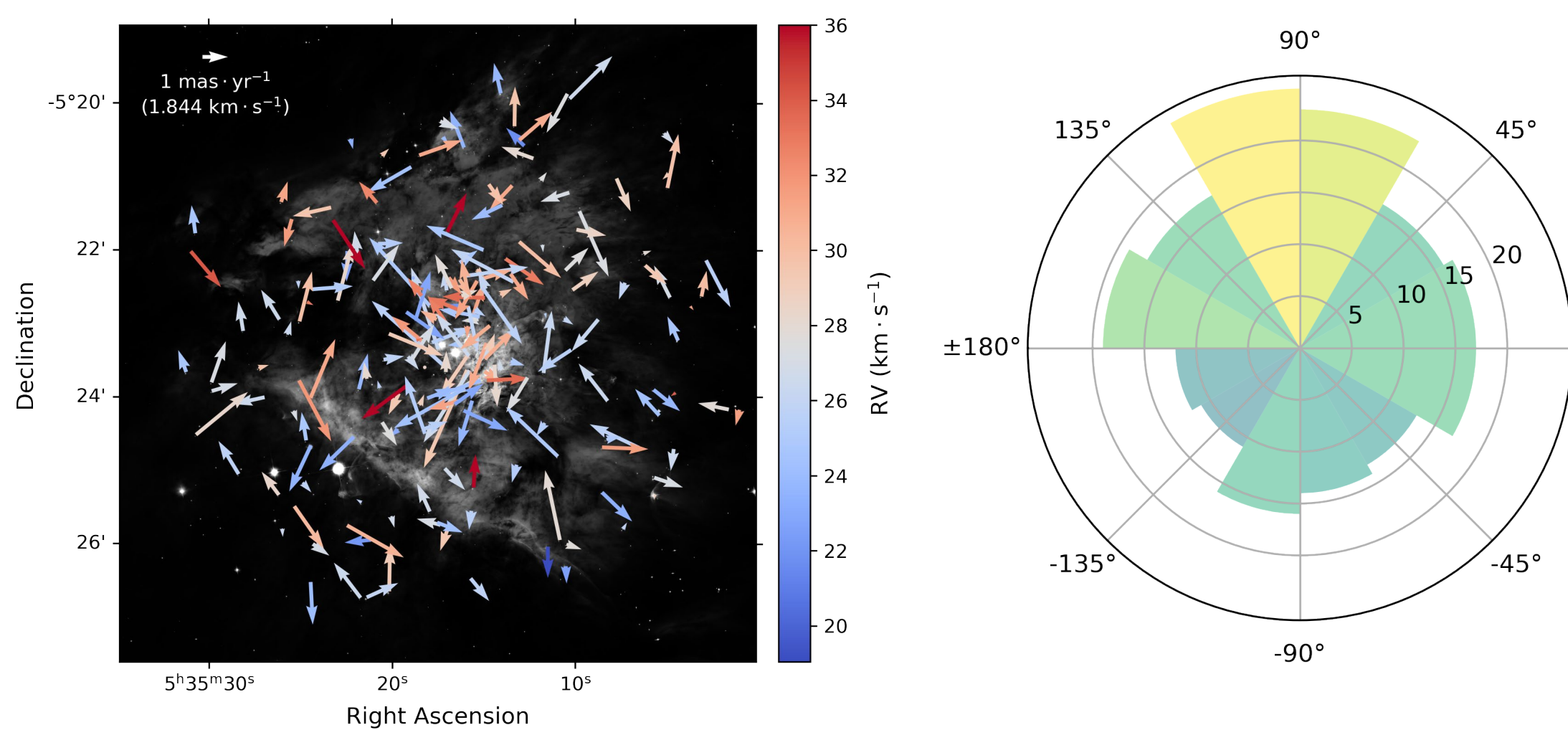


Fig. 4. Left: 3-D velocities of sources. Arrows represent proper motions and colors represent radial velocities. Right: Direction distribution between transverse velocity and displacement from the ONC center.

According to hydrodynamical simulations, stars can form from gravitational fragmentation in gas filaments infalling towards the cluster<sup>1</sup>. The high velocities of fast-moving stars precludes further accretion from the gas. Therefore, high velocity stars will have a lower mass. This negative correlation is observed in the ONC, indicating that the initial mass of forming stars indeed depend on their kinematic state.

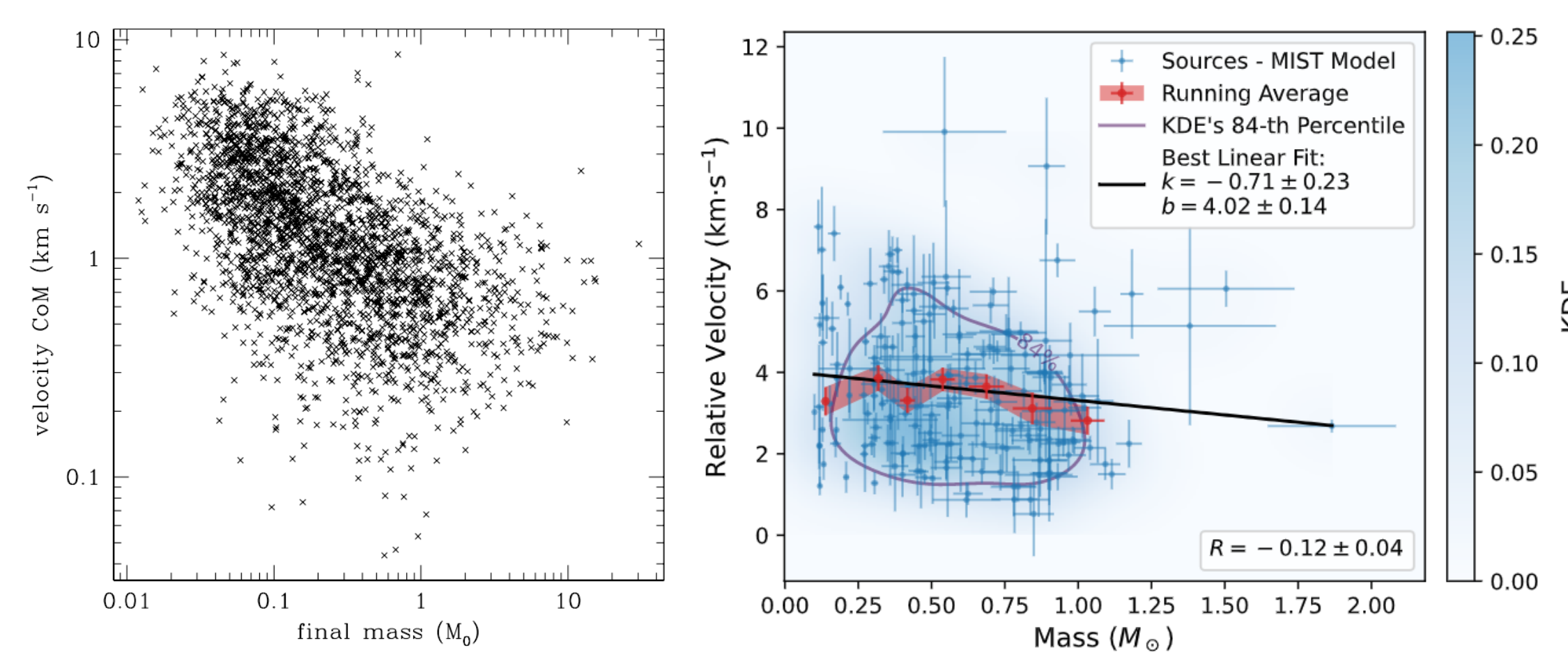


Fig. 5. Left: Relative velocity w.r.t. center of mass vs mass at the end of a hydrodynamical simulation<sup>11</sup>. Right: Observed relative velocity w.r.t. 0.1 pc neighbors vs mass interpolated from the MIST model.

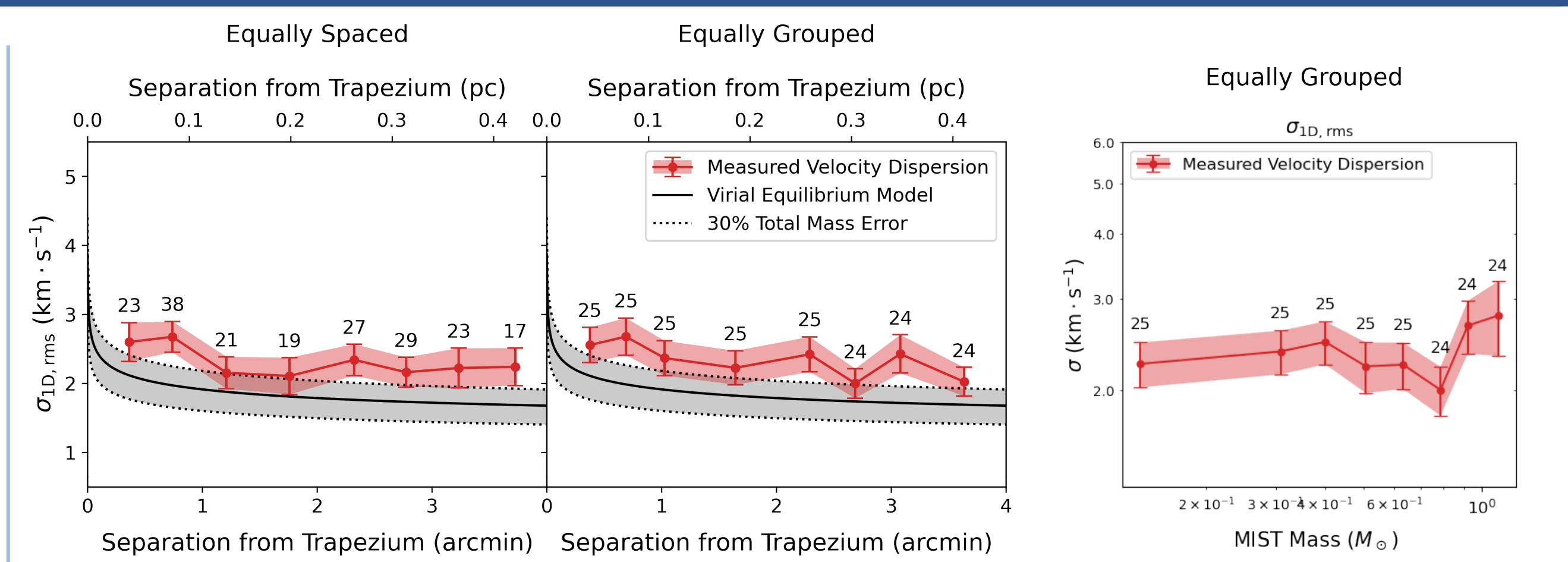


Fig. 6. Measured velocity dispersion (red) and virial equilibrium model prediction (gray) as a function of separation from the ONC center. Sources are binned with equal spacing or equal numbers in a group in left and right column respectively.

Fig. 7. 1-D velocity dispersion as a function of stellar mass. Sources are binned equally grouped.

**Fig. 6** shows the measured velocity dispersion as a function of separation from the ONC center:  $\sigma_{RA} = 1.71 \pm 0.09$  km/s,  $\sigma_{DE} = 2.08 \pm 0.11$  km/s,  $\sigma_{RV} = 2.98 \pm 0.15$  km/s, and  $\sigma_{1D} = 2.32 \pm 0.08$  km/s. The prediction of the virial equilibrium model<sup>12</sup> which assumes a virialized ONC is:  $\sigma_{equilibrium} = 1.73$  km/s. This implies that the ONC is not yet fully virialized yet. This is crucial as the negative trend in **Fig 5**. will be washed away if it were virialized.

We further prove that the downward trend is not a result of energy equipartition due to gravitational interactions, as the velocity dispersion will be inversely correlated to the square root of mass, or equivalently a minus one-half slope in log-log scale, which is not observed as in **Fig. 7**.

## Discussion and Takeaways

A discrepancy is identified between NIRSPA0 and APOGEE effective temperatures, as **Fig. 8** shows, possibly due to bias between K- and H-band. **Fig.9** shows the simulation on how offsetting the NIRSPA0 teff by the median difference affects the slope. The negative trend is mostly preserved under the offset. The simulated affect from binarity is shown in **Fig. 10**. A binary fraction of  $\geq 65.8\%$  is required to address the higher value of measured  $\sigma_{RV}$ , inconsistent with literature values.

### Takeaways:

ONC is supervirial. Stars form in gravitational fragmentation.

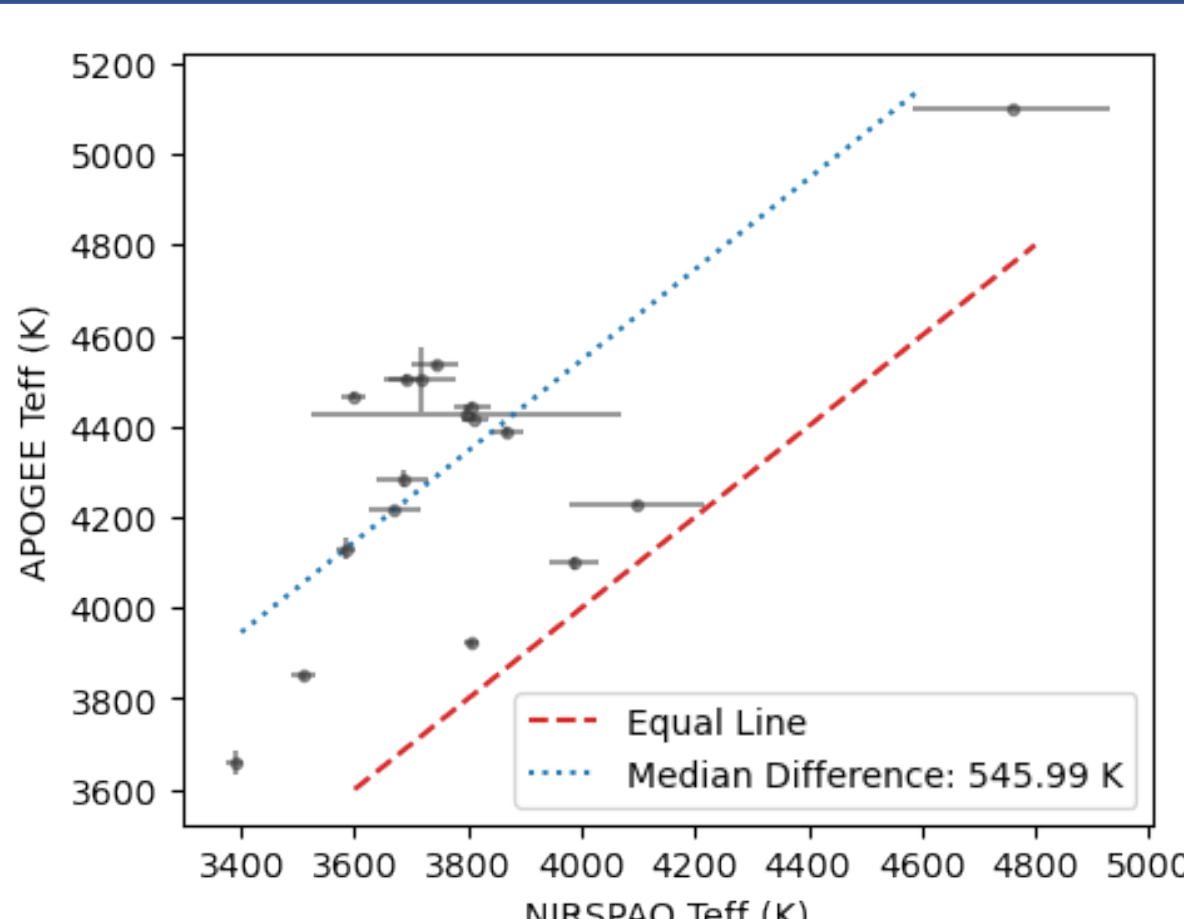


Fig. 8. Discrepancy in Teff between NIRSPA0 and APOGEE.

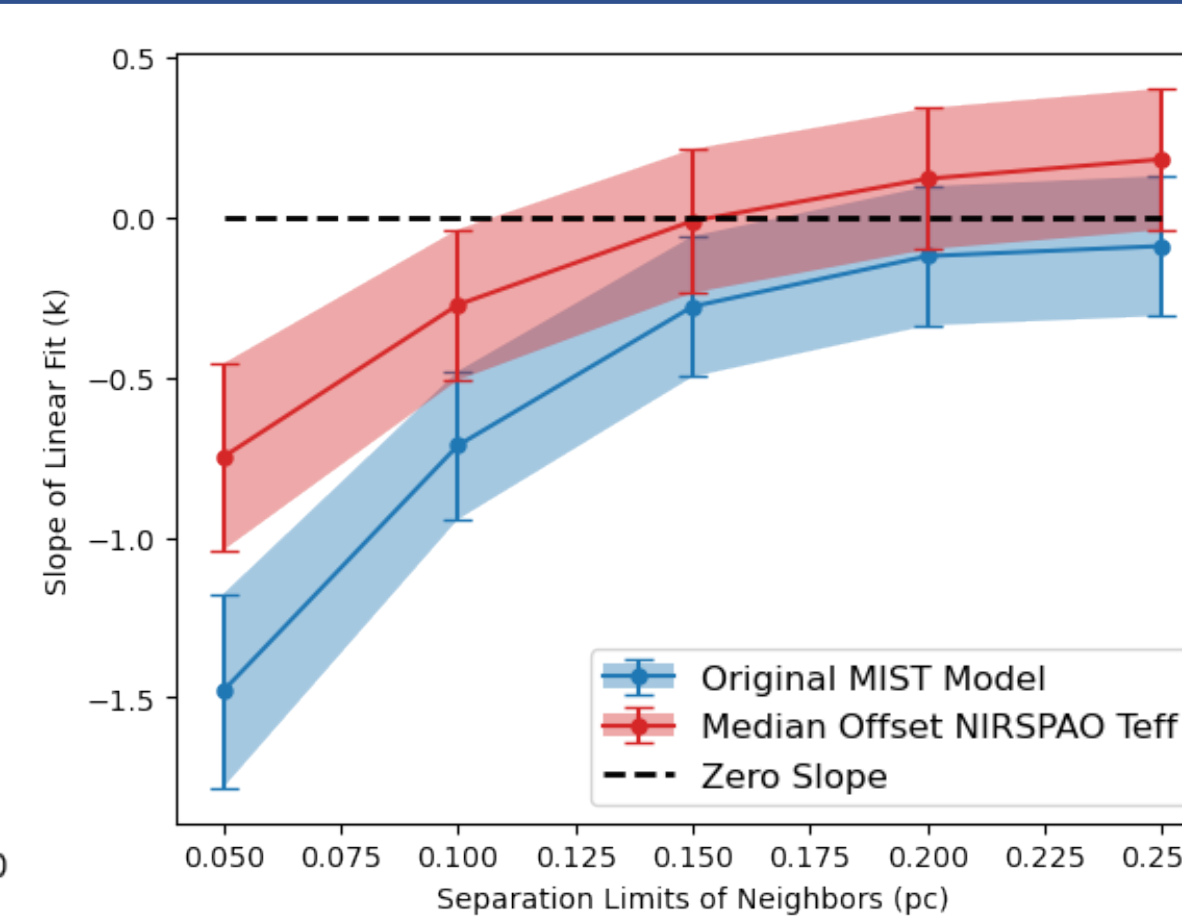


Fig. 9. Slope of linear fit as a function of separation limits of neighbors.

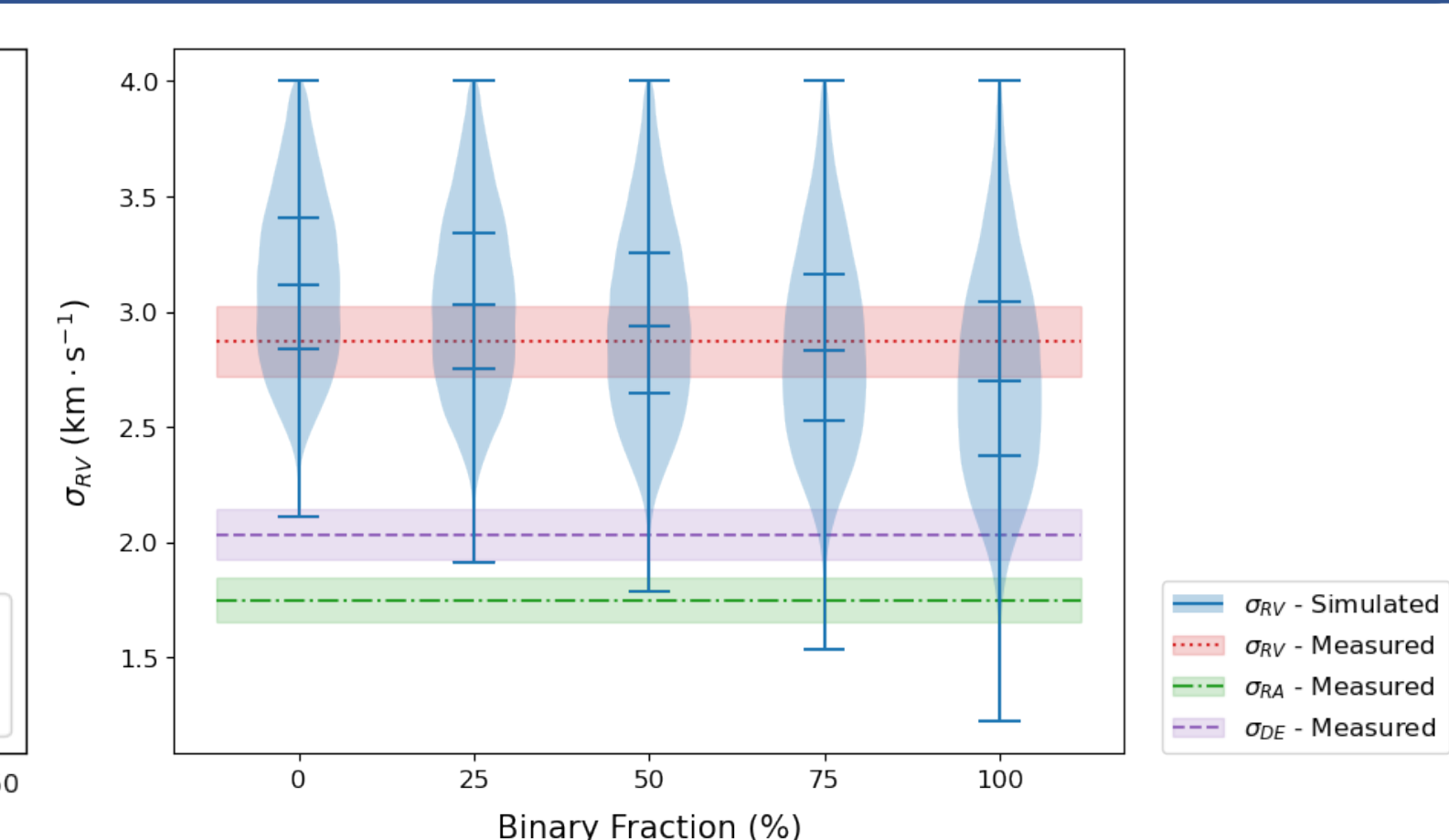


Fig. 10. Simulated and measured 1-D velocity dispersion assuming different binary fractions.

## Reference and Acknowledgement

- [1]. Bonnell, I. A., et al. 2008, MNRAS, 389, 1556. [6]. Kounkel, M. et al., 2018, AJ, 156, 3. [11]. Hsu, C.-C., et al., 2021, ApJS, 257, 45. [16]. Hillenbrand, L. A. 1997, AJ, 113, 1733.
- [2]. Hillenbrand & Carpenter 2000, ApJ, 540, 236. [7]. McLean, I. S., et al., 1998, SPIE, 3354, 566. [12]. Choi et al., 2016, ApJ, 823, 102.
- [3]. Theissen, C. A., et al., 2022, ApJ, 926, 141. [8]. McLean, I. S., et al., 2000, SPIE, 4008, 1048. [13]. Baraffe et al., 2015, A&A, 577, A42.
- [4]. Kim, D., et al., 2019, AJ, 157, 109. [9]. Husser, T. O., et al., 2013, A&A, 553, A6. [14]. Feiden et al., 2016, A&A, 593, A99.
- [5]. Majewski, S. R., et al. 2017, AJ, 154, 94. [10]. Hsu, C.-C., et al., doi: 10.5281.zenodo.4765258 [15]. Palla & Stahler, 1999, ApJ, 525, 772.

### Acknowledgement

We acknowledge the W. M. Keck Observatory, the LSST Data Science Fellowship Program, and everyone who has helped with this project.